SWIRL FLUID FLOW NOZZLE: A SOLUTION FOR FLUID JET POLISHING PROCESS

A.M. Najib[1] and D. Waechter[2]

[1]Faculty of Manufacturing Engineering,
Universiti Teknikal Malaysia Melaka, Hang Tuah Jaya, 76100 Durian Tunggal, Melaka, Malaysia.

[2]Fraunhofer Institute for Production Technology IPT,
Steinbachstrasse 17, Aachen, Germany.

Corresponding Author's Email: [1]najibali@utem.edu.my

Article History: Received 8 July 2020; Revised 15 February 2021; Accepted 16 April 2021

ABSTRACT: The Fluid Jet Polishing is one of emerging technology for fabrication of precision optics and medical implants. The current sub-aperture fluid jet polishing uses a canonical shaped nozzle which produces inequalities of surface removal. This study aims to present an alternative method using swirl nozzle design in order to eliminate the disadvantage of a ring-shaped influence function resulting from the fluid jet polishing using the conventional conical nozzle. The fluid jet flow of the conventional nozzle and swirl flow nozzle were investigated using numerical simulation. The jet profile and its parameter near the impact wall constitute a significant point of interest. The results indicated that particles and fluid exiting the nozzle at circumferential velocity improve the material removal characteristics during the polishing process. The study concluded that the nozzle with swirl flow resulted in a bell-shaped velocity profile near the impact wall, which provide a significant improvement in the polishing process using the fluid jet.

KEYWORDS: *Fluid Jet Polishing; Abrasive Water Jet; Computational Fluid Dynamics (CFD); Multiphase Flow; Nozzle*

1.0 INTRODUCTION

As optical design becomes more complex in geometries, new alternative processes are searched and continuously developed. Fluid Jet Polishing (FJP) using abrasive water jet is a newcomer in this field,

and it gives a significant advantage in sub-aperture polishing methods since there will be no tool wear. FJP is a shaping and finishing technique that was initially studied by Faehnle [1-2]. The material removal and polishing effect are depending on the impact power of the pressurized jet containing abrasives with the surface [3-4]. The jet power is created by a pump, pushing a given volume of water into the nozzle, which determines the final propagation.

FJP operates at lower pressure compared to abrasive water jet cutting. Abrasive Slurry Jet (ASJ) cutting systems operate at a pressure typically at several hundreds of bar [1] in contrast to approximately 20 bar in the FJP. The effect of nozzle pressure on material removal rate indicates that the material removal rate increase after a certain absolute threshold pressure [5-6]. The shape of the footprint, which creates by the jet on the surface, so-called influence function, determines the process capabilities and the resulting surface quality. Therefore, the shape of the nozzle is essential for controlling the influence function.

Generally, the nozzle designs are classified base on the working principle. A typical nozzle design bases on shear flow principle, where the fluid and particle stream along the axis as it enters the nozzle inlet and keeps flowing and accelerating until it is projected out of the nozzle. Typically, the nozzle has a conical shape. However, the influence of different nozzle geometries, such as a rectangular shape nozzle or different other shapes was studied by Rahman et al. [7]. Numerical simulation model of a conical nozzle to study inner flow field inside cyclone separator was established by Hamdy et al. [8]. In some designs, abrasive particles are injected to the fluid stream from different feed line, and the feed rate of the abrasive particles can be varied. However, these designs are mostly found in the nozzle used for water jet cutting.

A simulation of the 3D model of nozzle head able to trace two-phase field flows inside the abrasive water jet [9]. A study for water jet cutting shows that as the mass flow rate of the particle is increased, the erosion will also increase. However, if the abrasive concentration is very high, then the efficiency of a jet could decrease as the water jet has to accelerate more particles through the smaller tube [10]. In the fluid jet polishing, abrasive particles are mixed in the tank, and the slurry is pumped to the nozzle. A typical concentration of the particle contents in the slurry is 5% to 10% [11]. In some design, the shape of the accelerating tube is extended from a conical-shaped nozzle to increase the velocity of the medium. It was found out that for a specific diameter and pressure, there is the optimum length where the velocity of the

particle is the highest [12]. The second type of nozzle is a nozzle that works with the swirl fluid flow principle. As an example, a coil-like shape in the nozzle exit enables the water to follow the contours of the threaded nozzle. In a study by Madhu and Balasubramanian [13], the jet polishing using swirling jet able to produce better quality compare to the process using a cone-shaped nozzle in composite machining application. Simulation studies of the abrasive water jet, particularly in the jet cutting application were conducted by many researchers [14-16] compared to the fluid jet polishing application.

The presented work aims to investigate the problem involving fluid jet polishing using the conical nozzle. A ring-shaped influence function where more material is removed at the edge compared to the centre was undesirable in the fluid jet polishing process. Up to date, there is still limited study on the swirl flow nozzle, especially in a fluid jet polishing application. In this study, a finite volume method with discrete phase model was established using ANSYS Fluent solver, and design of the swirl nozzle was investigated as an improvement for the symmetrical influence function of the removal profile.

2.0 METHODS: CFD MODEL FORMULATION

The principal governing equations used to form the numerical simulation model and the pre-processing information, including geometrical model, material data and boundary conditions for the simulation study were presented. The problem involves three domains: particle, water and air. The multiphase volume of fluid (MVOF) with a combination of discrete phase model was chosen to simulate the flow of water and air. MVOF model was used for simulation of a fluid jet in air medium and used to track the surface of two immiscible fluids where the position of the interface between the jet flows of water through the air is of interest. The particles were defined in the discrete phase model (DPM). The fundamental governing equations for multiphase flow process was the Navier-Stoke equation; conversation of mass and momentum. The conservation of energy was not involved since the process is not temperature-dependent.

Rosin-Rammler method was used to describe the size distribution of abrasive particles. For slurry injection, the diameter size distribution was represented by the Rosin-Rammler expression. The complete range of diameter sizes was divided into an adequate number of discrete intervals. Each interval was represented by a mean diameter

for which trajectory calculations were performed. The graph in Figure 1 shows the percentage value of the corresponding particle's diameter, measured with a particle size analyzer (Mastersizer 2000 by Malvern Instruments). The presented work deals with the use of ceria abrasives. The particle sizes were tiny, and it tends to attract to each other to form bigger agglomerates. Therefore, the ultrasonic wave was used to scatter the particles of various sizes. Three probes of an equal amount were taken from the first sample and measured. The measured value of all probes and their average value was almost identical, as indicated in Figure 1.

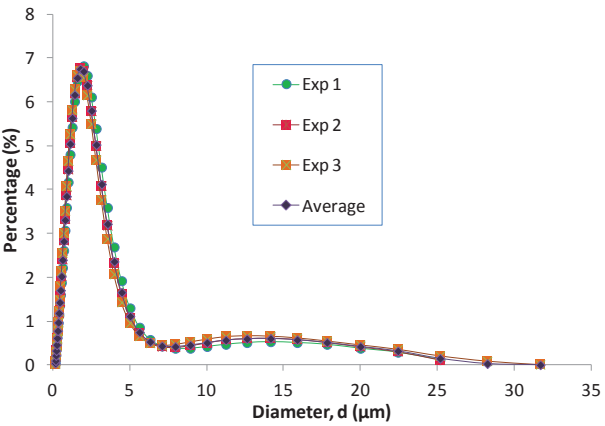

Figure 1: Particle distribution of cerium oxide

From the percentage of particle's diameter, a particle size distribution model was established to describe the size distributions of abrasive particles mathematically. The discrete circle line indicates the value from measurement, whereas the red line is the result of the mathematical expression. For the size distribution of the Rosin-Rammler method, the mass fraction of droplets of diameter greater than d is given by

$$Y_d = e^{-(\bar{d}/2.017)^n} \quad (1)$$

Symbol $\bar{d}$ is the size constant of average diameter equivalent to 2.017, and n is the distribution factor which is equal to 1.4. The value for diameter average $\bar{d}$ was obtained by noting the value of d at which $Y_d = 1/e$ or equivalent to 0.368. In the numerical simulation, the size distribution of particles was defined from the Rosin-Rammler method. Mass flow rate for each particle size was assumed constant. The equation from the Rosin-Rammler method mapped most of the particle's size distribution from the measurement values. The liquid-

gas interface in the geometry was considered as a steady-state phenomenon. Solid particle and liquid interaction were involved. A multiphase was implied, in which air was designated as the primary phase and water as the secondary phase. The particles were defined in the discrete phase model (DPM). Patching operation was required to fill the nozzle chamber with the secondary phase (air). The volume of fluid (VOF) with discrete phase modelling (DPM) was used for the model. The effect of gravity is very small and not accounted for in the simulation. Table 1 shows the geometrical and boundary conditions for the CFD analysis of the current nozzle. Figure 2 illustrates the design of the swirl fluid flow nozzle. The dark blue colour is the interior of the swirl nozzle, whereas the transparent blue colour shows the overall design of the swirl nozzle with a total length of 20.7 mm.

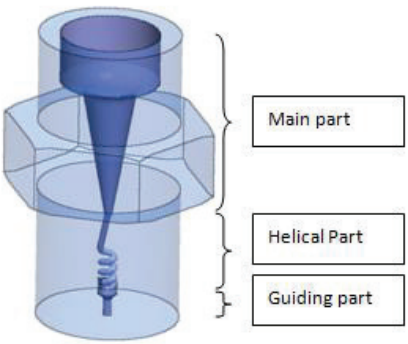

Figure 2: Exterior and interior of the new design of the swirl nozzle

Table 1: Geometrical, boundary parameters and turbulence model

Geometry / Boundary Condition / Turbulence Model	Parameters
Geometry	Nozzle length = 15 mm
	Orifice diameter = 4.7 mm
	Nozzle outlet diameter = 0.88 mm
	Stand-off distance = 10 mm
Boundary Condition	Abrasive velocity inlet = 0.747 m/s
	Abrasive density = 7280 kg/m^3 at 25°C
	Abrasive smallest diameter = 0.159 μm
	Abrasive mean diameter = 2.017 μm
	Abrasive biggest diameter = 28.5 μm
	Water inlet velocity = 0.747 m/s
	Density of fluid = 998 kg/m^3 at 25°C
	Viscosity of fluid = 0.001003 kg/ms at 25°C
	Density of air = 1.225 kg/m^3 at 25°C
	Viscosity of air = 1.7894e^{-5} kg/ms at 25°C
	Fluid solid fully-coupled and wall jet at impact wall
Turbulence Model	Realizable k-ε model
	C_2 = 1.9, σ_k = 1.0, σ_ε = 1.2

The upper part has the shape almost similar to the original nozzle. Sharp edges at the transition between cylindrical parts and tapered section were removed for better flow of fluid. The helical structure was designed to produce swirl fluid flow in a localized manner. The fluid was forced to flow through a certain number of helical turns before entering the guiding part. Guiding part was then used to direct the streams towards the target surface. Table 2 lists the design parameter implemented in the new helical nozzle model.

Table 2: Design Parameter of the new nozzle

Design Parameter	Values
Inlet diameter of the nozzle	7.0 mm
Outlet diameter of the nozzle	0.6 mm
Helical diameter	0.9 mm
Helical turns	2.5 turns
Helical pitch	0.75
Standoff distance	3 mm

In this model, the material data and boundary condition were defined. Due to highly swirling flows in the nozzle, the Reynolds stress model was implemented for the turbulence model. It was assumed that the particles follow the fluid streamline, and the velocity profile of fluid will have a significant impact on the fluid jet streamlines.

3.0 RESULTS AND DISCUSSION

Figure 3 shows the results of the velocity contour of numerical simulation in the propagation direction. Dark red colour represents the highest velocity, and the dark blue colour represents the lowest velocity. The fluid flows at the most top speed from the moment it been projected out until a certain distance before impact. At a near distance from the glass, the fluid profile behaves differently. Here, at the interface between air and fluid, and the average velocity was 14 m/s.

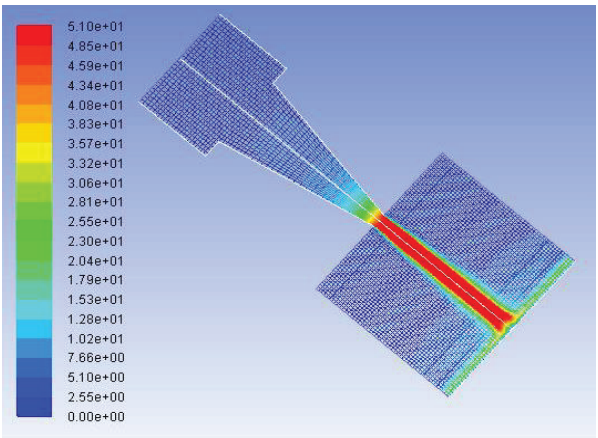

Figure 3: Velocity contour of the actual nozzle size

The nozzle diameter was varied, and its behaviour before impact was analyzed. The diameter of the current nozzle outlet is 0.88 mm, and the size of the orifice was varied from 0.5 mm to 1.35 mm. The diameter of the nozzle outlet is a crucial factor for the polishing performance. Increasing the outlet diameter reduces the slurry velocity, motion energy and hit power. Reducing the size of the orifice will force the volume of slurry to accelerate at a higher speed. Figure 4 shows the velocity magnitude measured in the axial direction from the moment the fluid start to accelerate until the moment of impact. The zero references in the graph are the tapered section of the nozzle. For all sizes of the orifice, the acceleration starts at the tapered section and reach its maximum velocity before it travelled at a constant value at a certain standoff distance. The velocity drops significantly to zero at the moment of impact. From the simulation, the average outlet velocity is around 49 m/s. As the outlet diameter increase to about 50%, the average velocity drops to more than half.

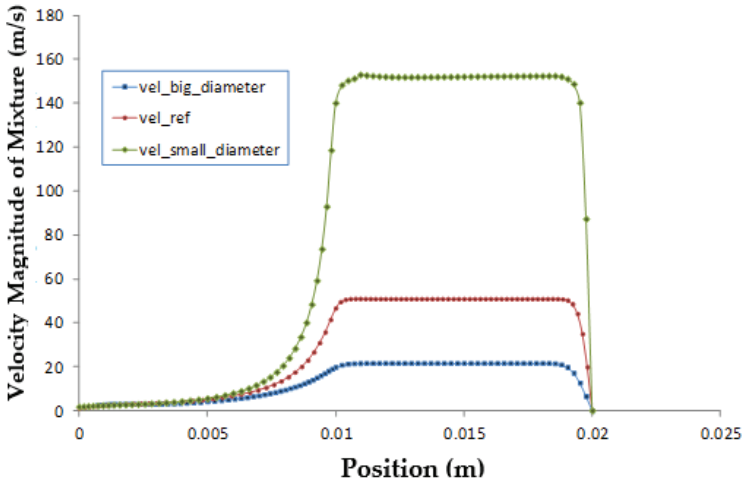

Figure 4: Velocity magnitude measured in the axial direction

Figure 5 illustrates the results of velocity profile measured at a distance near to the target wall, precisely at 1 mm and 0.5 mm from glass, respectively. At a distance of 1 mm from glass, the velocity profile of all diameter variation shows a similar pattern. For the reference diameter, the velocity at 1 mm before the impact measured at the centre of target point is 50 m/s. The velocity is constant for about 0.5 mm from the centre and decreases rapidly to 12 m/s. As the diameter of the orifice was changed to 1.35 mm, the velocity drops more than half to 20 m/s.

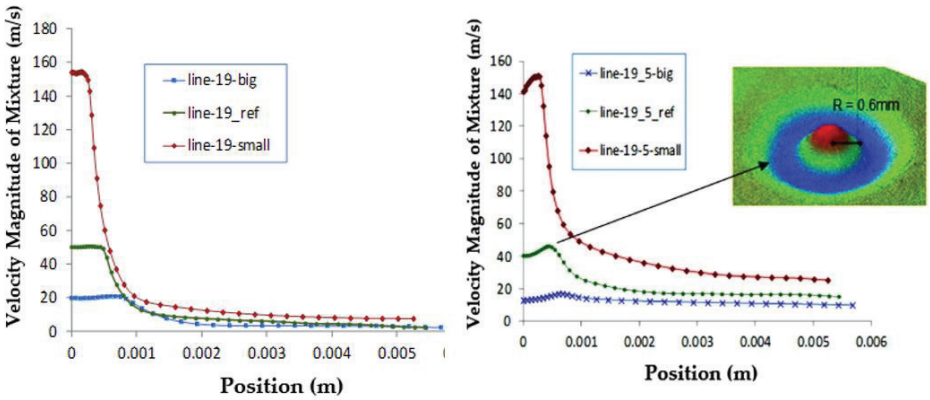

Figure 5: Velocity magnitude plot vs radial distance at (a) 1 mm and (b) 0.5 mm from glass

The velocity magnitude is less at the centre compared to a certain radial distance. At 0.6 mm from the centre of impact, the velocity is 5.7 m/s higher compare to the axial velocity. Figure 5(b) shows the result of the

numerical simulation of velocity magnitude measured at 0.5 mm from the glass and its radial direction. The result shows that the value of the velocity at the middle is lower compare to its neighbouring distance. For actual diameter, the velocity in the middle at a distance 0.5 mm from glass is 40 m/s. At 0.6 mm from the centre, it increases up to 5.7 m/s more and starts to decelerate and at a distance more than 2 mm from the centre, the value converges at a velocity 17 m/s. For nozzle diameter of 1.35 mm, the velocity at the centre is 4 m/s less from the peek point whereas for nozzle diameter of 0.5 mm, the velocity at the centre is 8 m/s less from the peak value.

Figure 6 illustrates the radial distribution of the axial velocity of the swirl fluid flow nozzle measured at 0.5 mm from workpiece of a surface. The zero references in the graph are the central axis, and it shows that the peak velocity is precisely at the centre. At 0.5 mm from the surface, the average velocity is 20 m/s. The result shows that helically shaped nozzle able to focus the water volume to the focus area and has a symmetrical velocity profile near the area of impact. This effect is significant to achieve deeper material removal at the centre compared to the edges.

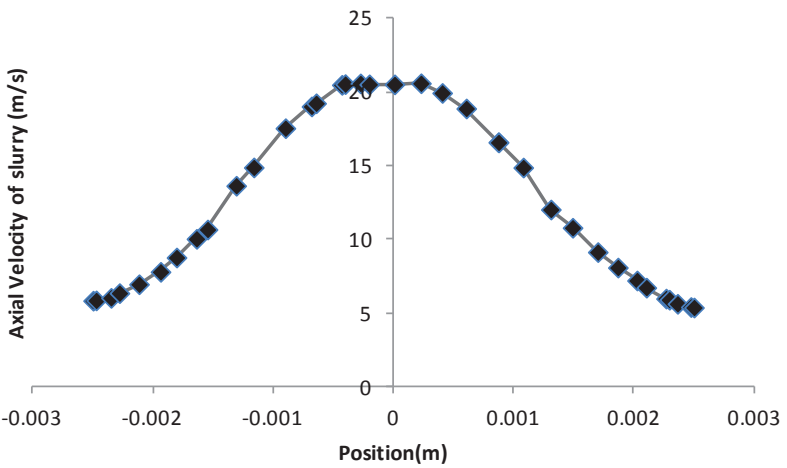

Figure 6: Radial distribution of axial velocity measured at 0.5 mm from the workpiece

The velocity profile from the swirl nozzle displays the potential of significant improvement compared to the conical nozzle. The result shows that the highest velocity occurred at the centre, which able to alter the material removal function at the centre. The implementation of a swirl fluid flow through the nozzle was proved to be useful in

removing the centre of the jet area and improved the influence function of the targeted area. A recent study related to the swirl fluid flow mechanism is reported by Kheradmand et al. [17]. The study showed that the swirl flow mechanism can indeed improve the surface roughness and use for surface modification. However, the study used a rotating inlet flow to produce the swirl flow mechanism, which slightly differs from the mechanism presented in this study.

4.0 CONCLUSION

The result from the numerical analysis indicates that the swirl fluid flow nozzle able to eliminate the ring-shaped influence function compare to the conventional cylindrical jet which work bases on shear flow principle to produce a U-shaped influence function. The velocity of the slurry at the centre is higher compared to its radial velocity and the fluid flow out of the swirl design is proved able to remove the material with its deepest part in the centre. It contributed to a significant improvement to the process, and the current problem with a ring-shaped contour on the surface using the conical nozzle can be solved using the swirl fluid flow. Other than that, the velocity magnitude of fluid dropped significantly as the function of the nozzle standoff distance. Therefore, a standoff distance of less than 10 mm is recommended for the swirl fluid flow. For future work, the design of the alternative swirl fluid flow nozzle such as abrasive fluid through a threaded nozzle or rotated nozzle should be further investigated.

ACKNOWLEDGEMENTS

The authors acknowledge the financial and support from the Ministry of Higher Education (MoHE), Universiti Teknikal Malaysia Melaka (UTeM) (RACER/2019/FKP-COSSID/F00409) and Fraunhofer Institute for Production Technology - Fraunhofer IPT (Germany).

REFERENCES

[1] O.W. Faehnle, “Shaping and finishing of aspherical optical surfaces”, Ph.D dissertation, Delft University of Technology, Delft, Netherlands, 1998.

[2] O.W. Faehnle, H. Van Brug, and H.J. Frankena, “Fluid jet polishing of optical surfaces”, *Applied Optics,* vol. 37, no. 28, pp. 6771-6773, 1998.

[3] R. Melentiev and F. Fang, "Theoretical study on particle velocity in micro-abrasive jet machining", *Powder Technology*, vol. 344, pp. 121-132, 2019.

[4] J. Poláček and E. Janurová, "Impact of pressure of surrounding medium on plain water jet cutting of rocks", *The International Journal of Advanced Manufacturing Technology*, vol. 90, no. 5, pp. 2185-2191, 2017.

[5] Z. Guo, T. Jin, L. Ping, A. Lu, and M. Qu, "Analysis on a deformed removal profile in FJP under high removal rates to achieve deterministic form figuring", *Precision Engineering,* vol. 51, pp. 160-168, 2018.

[6] F. Klocke, T. Schreiner, M. Schüler, and M. Zeis, "Material removal simulation for abrasive water jet milling", *Procedia CIRP*, vol. 68, pp. 541-546, 2018.

[7] M.S. Rahman, G.F.K. Tay, and M.F. Tachie, "Effects of nozzle geometry on turbulent characteristics and structure of surface attaching jets", *Flow, Turbulence and Combustion*, vol. 103, no. 3, pp. 797-825, 2019.

[8] O. Hamdy, M.A. Bassily, H.M. El-Batsh, and T.A. Mekhail, "Numerical study of the effect of changing the cyclone cone length on the gas flow field", *Applied Mathematical Modelling*, vol. 46, pp. 81-97, 2017.

[9] U. Prisco and M.C. D'Onofrio, "Three-dimensional CFD simulation of two-phase flow inside the abrasive water jet cutting head", *International Journal for Computational Methods in Engineering Science and Mechanics*, vol. 9, no. 5, pp. 300-319, 2008.

[10] M.G. Mostofa, K.Y. Kil, and A.J. Hwan, "Computational fluid analysis of abrasive waterjet cutting head", *Journal of Mechanical Science and Technology*, vol. 24, no. 1, pp. 249-252, 2010.

[11] O.W. Faehnle and H. Van Brug, "Finishing of optical materials using fluid jet polishing", in 14th American Society for Precision Engineering (ASPE) Annual Meeting, Monterey, California, 1999, pp. 509-512.

[12] G. Hu, W. Zhu, T. Yu, and J. Yuan, "Numerical simulation and experimental study of liquid-solid two-phase flow in nozzle of DIA jet," in IEEE International Conference on Industrial Informatics, Daejeon, South Korea, 2008, pp. 1700-1705.

[13] S. Madhu and M. Balasubramanian, "Effect of swirling abrasives induced by a novel threaded nozzle in machining of CFRP composites", *The International Journal of Advanced Manufacturing Technology*, vol. 95, no. 9, pp. 4175-4189, 2018.

[14] X. Miao, M. Wu, Z. Qiang, Q. Wang, and X. Miao, "Study on optimization of a simulation method for abrasive water jet machining", *The International Journal of Advanced Manufacturing Technology*, vol. 93, no. 1, pp. 587-593, 2017.

[15] L.H. Guo, S.S. Deng, and X. Yang, "Numerical simulation of abrasive water jet cutting chemical pipeline based on SPH coupled FEM", *Chemical Engineering Transactions*, vol. 51, pp. 73-78, 2016.

[16] Z. He, S. Zhao, C. Li, D. Li, Y. Zhang, T. Fu, and H. Yu, "Numerical investigation of surface topography and residual stress after abrasive water jet sequential peening (AWJSP)", *Machining Science and Technology*, vol. 24, no. 4, pp. 592-620, 2020.

[17] S. Kheradmand, M. Esmailian, and A. Fatahy, "A novel approach of magnetorheological abrasive fluid finishing with swirling-assisted inlet flow", *Results in Physics*, vol. 6, pp. 568-580, 2016.